Mathematical Population Studies, 22:71–79, 2015

ISSN: 0889-8480 print/1547-724X online
DOI: 10.1080/08898480.2014.925344

Routledge
Taylor & Francis Group

MIXED-MODE OSCILLATIONS DUE TO A SINGULAR HOPF BIFURCATION IN A FOREST PEST MODEL

Morten Brøns
Department of Applied Mathematics and Computer Science, Technical University of Denmark, Lyngby, Denmark

Mathieu Desroches and Martin Krupa
Inria Paris-Rocquencourt Research Centre, Domaine de Voluceau, Le Chesnay, France

In a forest pest model, young trees are distinguished from old trees. The pest feeds on old trees. The pest grows on a fast scale, the young trees on an intermediate scale, and the old trees on a slow scale. A combination of a singular Hopf bifurcation and a "weak return" mechanism, characterized by a small change in one of the variables, determines the features of the mixed-mode oscillations. Period-doubling and saddle-node bifurcations lead to closed families (called* isolas*) of periodic solutions in a bifurcation corresponding to a singular Hopf bifurcation.

Keywords: canards; forest pest model; mixed-mode oscillations; singular Hopf bifurcation; slow-fast systems

1. INTRODUCTION

Outbreaks of the spruce budworm *Choristoneura fumiferana* have been recorded regularly in the eastern United States since the early 19th century (Schultz, 2009). Budworms damage balsam fir and spruce and the outbreaks have severe economical consequences for the forest industry (Kucera and Orr, 1980). Ludwig et al. (1978) dealt with population dynamics including interaction between trees and budworms. They found relaxation oscillations: the populations move slowly, approaching quasi-equilibrium states, briefly interrupted by periods of fast dynamics corresponding to budworm outbreaks. The fact that the budworm population grows on a much faster scale than the trees implies that the model has an inherent slow-fast structure where this kind of dynamics is expected. Relaxation oscillations are also observed in other forest pest models (Berryman et al., 1987; Muratori and Rinaldi, 1989; Rinaldi and Muratori, 1992; Antonovsky et al., 1990; Gragnani et al., 1998; Buřič et al., 2006).

We consider again the three-variable forest pest model of Rinaldi and Muratori (1992), developing on Brøns and Kaasen (2010), who showed the existence of

Address correspondence to Martin Krupa, Inria Paris-Rocquencourt Research Centre, Domaine de Voluceau, Rocquencourt BP 105, 78153, Le Chesnay cedex, France. E-mail: maciej.p.krupa@gmail.com

mixed-mode oscillations in this model. The population of trees is structured in young and old trees to capture the fact that the pest mainly feeds on old trees. In dimensionless variables, the equations are

$$\begin{cases} x'(t) = a_1 y(t) - a_2 x(t) - a_3 \dfrac{x(t)z(t)}{a_4 + x(t)}, \\ \delta y'(t) = a_5 x(t) - (a_6(x(t) - a_7)^2 + a_8 + \delta a_1) y(t), \\ \varepsilon z'(t) = \left(-a_9 - a_{10} z(t) - \dfrac{a_{11}}{a_{12} + z(t)} + a_{13} \dfrac{x(t)}{a_4 + x(t)} \right) z(t), \end{cases} \tag{1}$$

where $x(t)$ is the population size of old trees, $y(t)$ is the population size of young trees, and $z(t)$ is the pest population size at time t. The time scale for the old trees is taken as 1, δ is the time scale of young trees, and ε is the time scale of the pest (Rinaldi and Muratori, 1992).

Eq. (1) has a special structure given by the invariant plane $\{z = 0\}$ and the invariant line $\{x = y = 0\}$. The relevant part of the space is the invariant half-space $\{z > 0\}$, corresponding to the condition that the pest population size is always positive. Eq. (1) is similar to systems with symmetry in which invariant spaces, especially invariant hyperplanes, often play an important role.

Rinaldi and Muratori (1992) considered the case $\varepsilon \ll \delta \ll 1$. Based on singular perturbation theory, inequalities with parameters guarantee the existence of relaxation oscillations. Brøns and Kaasen (2010) considered Eq. (1) for a fixed small ε in the limit $\delta \to 0$. Fenichel theory (1979) allows a reduction to a two-dimensional system on an attracting invariant manifold close to $y' = 0$. The reduced system has a canard explosion (Benoît et al., 1981). When a parameter is varied through a Hopf bifurcation, a limit cycle appears. It grows into relaxation over a narrow parameter interval. Biologically, the combination of a Hopf bifurcation and a canard explosion corresponds to the transition from an equilibrium state where the forest is infected (i.e., the pest population $z \neq 0$) toward a periodic state with budworm outbreaks.

The canard analysis is only valid for δ sufficiently small. As δ increases, the two-dimensional invariant manifold breaks down, allowing for three-dimensional mixed-mode oscillations (Desroches et al., 2012), that is, limit cycles with small and large oscillations and long periods (Figure 1c).

Mixed-mode oscillations occur in systems with folded singularities (Brøns et al., 2006). We will show that a folded node exists in Eq. (1) and does not determine the mixed-mode oscillations for the parameters considered in Brøns and Kaasen (2010). Rather, a combination of a singular Hopf bifurcation (Guckenheimer, 2008; Guckenheimer and Meerkamp, 2012) and a "weak return" mechanism, partly due to the smallness of δ (Section 2) are the key factors of the mixed-mode dynamics. We analyze Hopf and period-doubling bifurcations in Eq.(1) and the presence of folded singularities, and we show that mixed-mode oscillations are due to a singular Hopf bifurcation. It is more complex than what would be expected from a folded node scenario.

We keep the same set of parameter values as in Brøns and Kaasen (2010): all dimensionless a_k 's are equal to 1 except $a_2 = 0.2$, $a_3 = 7$, $a_{11} = 2$, $a_{13} = 5$, and a_5 and δ, which will be varied. We fix $\varepsilon = 0.001$.

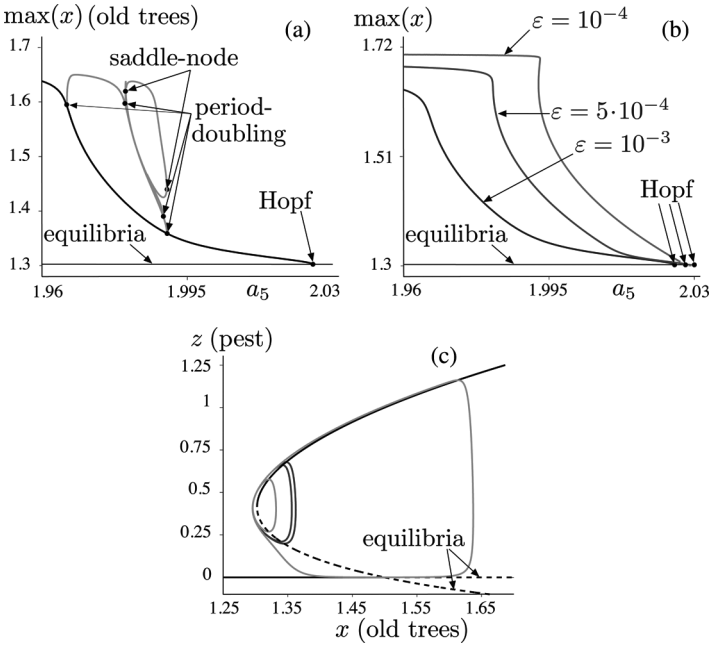

Figure 1. Bifurcation diagram of Eq. (1) in parameter a_5 for $\delta = 0.3$. Panel (a): the curve of equilibria is shown in black; the maximum in x along the branch of limit cycles as well as along period-doubled branches and along an *isola* of mixed-mode oscillations is shown in grey; black dots indicate Hopf, period-doubling as well as saddle-node bifurcations encountered during the computation. Panel (b) shows the same branch of limit cycles computed with three different decreasing values of ε: 10^{-3}, $5 \cdot 10^{-4}$, and 10^{-4}. This shows the explosive aspect of the branch when ε gets closer to the singular limit. Panel (c) shows a small-amplitude period-doubled limit cycle for $a_5 \approx 1.990$ and 1^1 mixed-mode oscillation for $a_5 \approx 1.976$, along the period-doubled branch displayed in (a), in projection onto the (x, z)-space. The projection of the critical manifold is represented with its attracting (solid) and repelling (dotted) branches.

2. FEATURES OF EQ. (1)

Eq. (1) defines a slow-fast system with two slow variables, x and y, and one fast variable z. The critical manifold S of this system is defined as the fast null surface, as:

$$S := \left\{ \left(-a_9 - a_{10} z - \frac{a_{11}}{a_{12} + z} + a_{13} \frac{x}{a_4 + x} \right) z = 0,\ z \in \mathbb{R}^+ \right\}. \tag{2}$$

S is the union of a folded surface C and the plane $\Pi := \{z = 0\}$ with C defined by

$$C := \left\{ x = \varphi(z) = \frac{a_4 \left(a_9 + a_{10} z + \frac{a_{11}}{a_{12}+z} \right)}{a_{13} - a_9 - a_{10} z - \frac{a_{11}}{a_{12}+z}},\ z \in \mathbb{R}^+ \right\}. \tag{3}$$

The surface C is S-shaped with "fold" curves:

$$F_{\pm} := \left\{ (x, y, z) \in C \mid z = \pm \left(\frac{a_{11}}{a_{10}} \right)^{\frac{1}{2}} - a_{12} \right\}. \tag{4}$$

The plane Π and the sets $\{z > 0\}$ and $\{z < 0\}$ are invariant for the flow. The mixed-mode oscillations observed by Brøns and Kaasen (2010) are contained in the half-space $\{z > 0\}$. The mixed-mode solutions have small oscillations near F_+, jump to the stable part of Π, evolve close to it, cross the instability line defined by $\Pi \cap C$, and evolve close to the unstable part of Π. The passage along Π corresponds to a simple delay phenomenon; the invariance of Π implies that the amount of time spent by the solution near the unstable part of Π is determined by the balance of attraction and expansion along Π. Π plays a similar role to that of the invariant line in Pokrovskii et al. (2008).

The dynamics would be different if the invariance of Π was broken for $\varepsilon > 0$, as a delay phenomenon would occur only near discrete parameter values due to the passage near a canard trajectory (Krupa and Szmolyan, 2001). An analogous effect is expected in systems with symmetry, which can change slow-fast dynamics.

In Eq. (1), the solution moves mainly in the x direction so that it returns to F_+ with approximately the same values of y. As $\delta = 0.3$ is still quite small, the solution is close to the y null-surface, which is the surface obtained by setting the right-hand side of Eq. (1) to 0. The y null-surface equation defines y as a function of x, independently of z. Hence the transition from any section $\{x = \text{const}\}$ back to itself through a global return results in a value of y very close to the initial one. We call this property "weak return."

3. NUMERICAL BIFURCATION ANALYSIS OF EQ. (1)

We use the software package Auto (Doedel et al., 2007) to perform a numerical bifurcation analysis of Eq. (1) in parameter a_5. Figure 1a shows some families of stationary and periodic attractors of Eq. (1) for a_5 varying in the interval [1.96, 2.03]. Computation shows that the unique nontrivial ($z_{eq} \neq 0$) equilibrium loses its stability after a Hopf bifurcation (H) at $a_5 \approx 2.025278$. This value depends on ε and is rather close to 1.987 chosen in Figure 2. A pair of period-doubling bifurcations along the branch of limit cycles born at the Hopf bifurcation modifies the stability of this branch. The branch of period-doubled cycles yields two other period-doubling bifurcations, which are likely to participate in cascades generating chaotic dynamics. Along each branch of periodic solutions—period one, two, and four shown in Figure 1—an explosion occurs, by which small cycles (small-amplitude period-2k cycles) grow into large-amplitude relaxation cycles (1^{2k-1} mixed-mode oscillations, i.e., a mixed-mode periodic solution with one large oscillation and $2k-1$ small oscillations per period). Figure 2 shows two different phase-space views of a mixed-mode oscillation. Certain families of mixed-mode oscillations form closed curves in the parameter space, also referred to as *isolas* (Golubitsky and Schaeffer, 1985). Such an *isola* is shown in Figure 1. Mixed-mode oscillations on this *isola* have a 1^2 pattern of oscillation. The relaxation cycles and the relaxation loop of mixed-mode oscillations are made possible by the second branch of the *critical manifold* C of Eq. (1), that is, the plane $\{z = 0\}$, which is

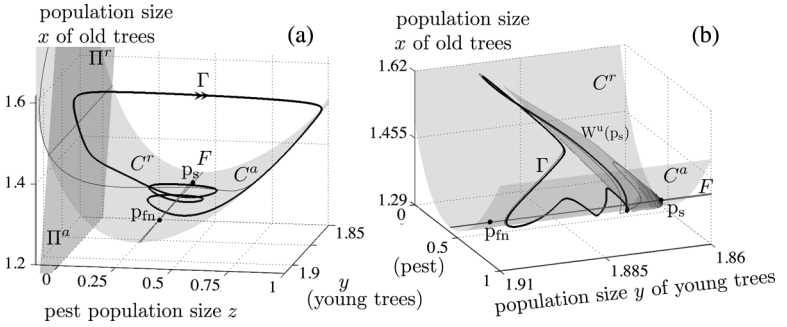

Figure 2. Panel (a): Mixed-mode oscillation of Eq. (1) and the critical manifold $C \cup \Pi$, formed by two components, each having attracting and repelling submanifolds. The black dots represent the folded node p_{fn} and the saddle-focus equilibrium p_s of the system. The non-fold component of the y null-cline of the desingularized reduced system and the z null-cline of the desingularized reduced system are also represented. Panel (b) shows an approximation of the two-dimensional unstable manifold $W^u(p_s)$ of p_s, which drives the behavior of the stable mixed-mode oscillation during the return.

attracting in the x-interval where the folded sheet of C is unstable (Section 2). This double canard effect—canard explosion giving a canard segment around a fold point of the critical manifold and delayed exchange of stability giving a second canard segment near a non-fold non-hyperbolic point of the critical manifold—was termed canard doublet in the context of Lotka-Volterra equations (Pokrovskii et al., 2008). This phenomenon is shown in Figure 1c. A period-doubled cycle and a 1^1 mixed-mode oscillation, computed on the branch of period-two cycles (Figure 1a) for very close values of a_5, are shown on top of the critical manifold. The explosive character of the branch of periodic solutions appears for small enough ε. Figure 1b presents the branch of period-one solutions computed for $\varepsilon = 0.001$, 0.0005, and 0.0001. The narrow range for a_5 on the horizontal axis brings evidence that the branch becomes nearly vertical as ε decreases to zero.

When continuing the rightmost period-doubling bifurcation of Figure 1 in both parameters a_5 and δ, we find a curve that is consistent with the boundary of the region of mixed-mode oscillations computed in Brøns and Kaasen (2010) by simulation (Figure 4, Brøns and Kaasen, 2010). Figure 3 compares both computations. The *isolas* of mixed-mode oscillations in the (a_5, δ) parameter plane are located within the curve of period-doubling bifurcations. This gives additional numerical evidence that the mixed-mode dynamics is confined to the narrow band (Brøns and Kaasen, 2010). The existence of mixed-mode dynamics in this model is related to period-doubling bifurcations followed by canard explosions for ε small enough.

4. SLOW-FAST ANALYSIS OF EQ. (1)

The mixed-mode oscillations oscillate around the fold curve $F_+ = F$, where we will focus our analysis (Figure 2). We define

$$\alpha := \left(\frac{a_{11}}{a_{10}}\right)^{\frac{1}{2}} - a_{12} \tag{5}$$

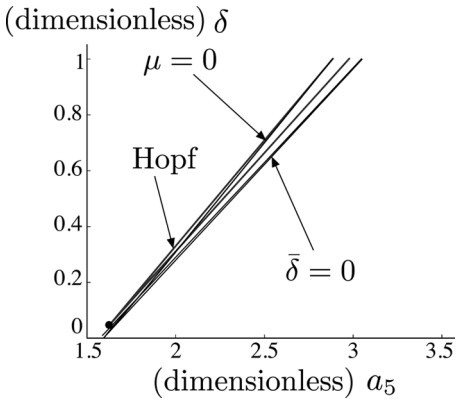

Figure 3. Locus of period-doubling bifurcations in the (a_5, δ)-plane computed using a numerical continuation routine, superimposed onto Figure 4 of Brøns and Kaasen (2010). The curve of period-doubling bifurcations is consistent with the boundary of the region where mixed-mode oscillations appear by direct simulation of Eq. (1). On the left, the black curves correspond to the locus of Hopf bifurcations and the solution of the equation $\mu = 0$ (almost superimposed); on the right, they correspond to the solution of the equation $\bar{\delta} = 0$, where $\bar{\delta}$ is the distance of the return to the strong canard.

in order to show that mixed-mode oscillations in Eq. (1) originate from a singular Hopf bifurcation.

Consider the set of parameters of Brøns and Kaasen (2010): $a_5 = 1.987$ and $\delta = 0.3$ as in Figure 3 (e)-(f) of Brøns and Kaasen (2010). The periodic attractor of Eq. (1) for these values is a mixed-mode oscillation of pattern 1^2 (one large-amplitude oscillation and two small-amplitude oscillations).

The desingularized reduced system

$$\begin{cases} \delta y'(t) = \varphi_z(z(t))(a_5\varphi(z(t)) - (a_6(\varphi(z(t)) - a_7)^2 + a_8 + \delta a_1)y(t), \\ z'(t) = a_1 y(t) - a_2\varphi(z(t)) - a_3\dfrac{\varphi(z(t))z(t)}{\varphi(z(t)) + a_4} \end{cases} \tag{6}$$

implies that Eq. (1) possesses a folded node, that is, a node equilibrium of the desingularized reduced Eq. (6) lying on the fold curve F. Hence, a folded node corresponds to $\varphi'(z_{\mathrm{fn}}) = 0$, then $z_{\mathrm{fn}} = \alpha = \left(\frac{a_{11}}{a_{10}}\right)^{\frac{1}{2}} - a_{12}$. Finally, the coordinates of the folded node are:

$$\begin{cases} x_{\mathrm{fn}} = \varphi(\alpha) = \dfrac{a_4\left(a_9 + 2(a_{10}a_{11})^{\frac{1}{2}} - a_{10}a_{12}\right)}{a_{13} - \left(a_9 + 2(a_{10}a_{11})^{\frac{1}{2}} - a_{10}a_{12}\right)} \\ y_{\mathrm{fn}} = \dfrac{x_{\mathrm{fn}}}{a_1}\left(a_2 + a_3\dfrac{z}{x_{\mathrm{fn}} + a_4}\right) \\ z_{\mathrm{fn}} = \alpha. \end{cases} \tag{7}$$

Figure 2 shows that the folded node is not located at the center of the small-amplitude oscillations within the mixed-mode oscillation. Consequently, folded node theory fails to account for the dynamics of Eq. (1).

First, the mixed-mode oscillations are far away from the folded singularity and are close to a saddle-focus equilibrium. Second, small-amplitude oscillations are few with regard to what they should be according to folded node theory. These features of the trajectories are partly due to the proximity of a singular Hopf bifurcation. For all values of a_5, using a similar argument as in Szmolyan and Wechselberger (2001), we prove that Eq. (1) has a unique folded singularity given by Eq. (7). We change the coordinates, so that Eq. (1) becomes:

$$\begin{cases} x'(t) = \mu + Ax(t) + Bz(t) + \text{ higher order terms} \\ \delta y'(t) = x(t) - y(t) + \text{ higher order terms} \\ \varepsilon z'(t) = (-x(t) + \varphi(z(t)))(z(t) + \alpha), \end{cases} \tag{8}$$

where μ, A, and B are functions of the parameters $a_1, \ldots, a_{13}$, and δ. To change variables, we first replace $x(t)$ by $x(t)/(a_4 + x(t))$, then replace (x, y, z) by $(x - x_{\text{fn}}, y - y_{\text{fn}}, z - z_{\text{fn}})$, and rescale. For each $\mu > 0$, the origin is a folded node point and $\mu = 0$ corresponds to a singular Hopf bifurcation. The value of a_5 corresponding to $\mu = 0$ is $a_5 \approx 2.030596282$. We found this value by expanding the vector field about the folded node and calculating the value of a_5 for which the resulting Taylor expansion has its constant term vanishing, which corresponds to $\mu = 0$ in Eq. (8). The value of the Hopf bifurcation computed with Auto is $a_5 \approx 2.0252772146$ for $\varepsilon = 10^{-3}$, $a_5 \approx 2.0279173803$ for $\varepsilon = 5 \cdot 10^{-4}$, and $a_5 \approx 2.0300574958$ for $\varepsilon = 10^{-4}$.

For a singular Hopf bifurcation, near the folded singularity, there exists a center manifold, weakly unstable, with Hopf type dynamics (Guckenheimer, 2008), denoted by $W^u(p_s)$. For $\mu > 0$ very small, this center manifold corresponds to a saddle-focus point with a strongly stable real eigenvalue and a weakly unstable center direction. The trajectories passing near the folded singularity are attracted to the unstable center manifold of the saddle point and follow the dynamics on it. This implies that the small-amplitude oscillations are close to the saddle-focus equilibrium rather than remaining near the folded singularity.

The chaotic dynamics arises from the transition between the center manifold and the set of slow manifolds farther away from the fold line. By this mechanism, simple periodic orbits undergo a period-doubling cascade *en route* to chaos. Subsequently, complicated periodic orbits undergo canard explosions on one of their loops, growing to mixed-mode oscillations. This mechanism is not completely understood yet (Guckenheimer, 2008; Guckenheimer and Meerkamp, 2012) for generating mixed-mode oscillations. Figure 1 shows a transition from a period-doubled orbit to a 1^1 mixed-mode oscillation through a canard explosion.

The second feature of Eq. (1) shaping the mixed-mode oscillation trajectories is the weak return: y changes very little in the course of a global return. This implies that every trajectory returning through the global return is close to the strong canard, staying away from the central sector of the funnel corresponding to the maximal total number of small-amplitude oscillations (Brøns et al., 2006). As y in the fold region moves faster than x, the solution moves relatively fast toward $W^u(p_s)$ and then leaves the vicinity of the fold region (Figure 2b).

With regard to folded node theory, the maximal total number of small oscillations in a mixed-mode oscillation generated from a folded node comes from

$$s_{\max} = [\Psi(\mu)], \tag{9}$$

where $[\cdot]$ denotes the integer part and $\Psi(\mu)$ is a smooth function satisfying $\Psi(\mu) = O(1/\mu)$ (Wechselberger, 2005; Vo et al., 2010). Applying this to the case $a_5 = 1.987$ and $\delta = 0.3$ yields $s_{\max} = 27$, substantially above the actual value $s = 2$. This indicates that the folded node scenario does not explain the pattern of mixed-mode oscillations observed here.

5. CONCLUSION

We completed the analysis of mixed-mode oscillations done by Brøns and Kaasen (2010) for the forest pest model of Eq. (1). Eq. (1) provides an example where the generating mechanism is the singular Hopf bifurcation rather than the folded singularity. The folded node in the model is not decisive in shaping and organizing mixed-mode oscillations so that small-amplitude oscillations are fewer than what they should be under folded node theory (Brøns et al., 2006).

To understand the mixed-mode dynamics of Eq. (1), we located the folded singularity and the saddle-focus equilibrium of the full system, computed the eigenvalues at the equilibrium, and assessed the properties of the global return. The forest pest model for the chosen parameters is more kin to the singular Hopf bifurcation than to the folded node or folded saddle-node (Brøns et al., 2006; Guckenheimer, 2008; Krupa and Wechselberger, 2010; Guckenheimer and Meerkamp, 2012). In particular, Guckenheimer and Meerkamp (2012) pointed out the role of period-doubling bifurcations in the mixed-mode dynamics in a singular Hopf normal form in connection with canard explosion phenomena. We showed that, for small enough ε, the presence of mixed-mode oscillations in Eq. (1) owes to the explosion of small-amplitude period-$2n$ ($n \in N$) cycles born along a cascade of period-doubling bifurcations. This cascade involves a small-amplitude chaotic attractor. There are also orbits of period $2n+1$ located on *isolas* changing their large-amplitude oscillations through period-doubling bifurcations.

REFERENCES

Antonovsky, M. Y., Fleming, R. A., Kuznetsov, Y. A., et al. (1990). Forest-pest interaction dynamics: The simplest mathematical models. *Theoretical Population Biology*, *37*(2): 343–367.

Benoît, E., Callot, J. -L., Diener, F., et al. (1981). Chasse au canard. *Collectanea Mathematica*, *32*(1–2): 37–119.

Berryman, A. A., Stenseth, N. C., and Isaev, A. S. (1987). Natural regulation of herbivorous forest insect populations. *Oecologia*, *71*(2): 174–184.

Brøns, M. and Kaasen, R. (2010). Canards and mixed-mode oscillations in a forest pest model. *Theoretical Population Biology*, *77*(4): 238–242.

Brøns, M., Krupa, M., and Wechselberger, M. (2006). Mixed-mode oscillations due to the generalized canard phenomenon. In W. Nagata and S. R. Namachchivaya (Eds.),

Bifurcation Theory and Spatio-Temporal Pattern Formation. Volume 49 of Fields Institute Communications. Providence, RI: American Mathematical Society, 39–63.

Buřič, L., Klíč, A. and Purmová, L. (2006). Canard solutions and travelling waves in the spruce budworm population model. *Applied Mathematics and Computation*, *183*(2): 1039–1051.

Desroches, M., Guckenheimer, J., Krauskopf, B., et al. (2012). Mixed-mode oscillations with multiple time scales. *SIAM Review*, *54*(2): 211–288.

Doedel, E. J., Paffenroth, R. C., Champneys, A. R., et al. (2007). AUTO-07P: Continuation and bifurcation software for ordinary differential equations. Retrived from http://indy.cs.concordia.ca/auto

Fenichel, N. (1979). Geometric singular perturbation theory for ordinary differential equations. *Journal of Differential Equations*, *31*(1): 53–98.

Golubitsky, M. and Schaeffer, D. G. (1985). *Singularities and Groups in Bifurcation Theory* (Volume 1). New York: Springer-Verlag.

Gragnani, A., Gatto, M., and Rinaldi, S. (1998). Acidic deposition, plant pests, and the fate of forest ecosystems. *Theoretical Population Biology*, *54*(3): 257–269.

Guckenheimer, J. (2008). Singular Hopf bifurcation in systems with two slow variables. *SIAM Journal on Applied Dynamical Systems*, *7*(4): 1355–1377.

Guckenheimer, J. and Meerkamp, P. (2012). Unfoldings of singular Hopf bifurcation. *SIAM Journal on Applied Dynamical Systems*, *11*(4): 1325–1359.

Krupa, M. and Szmolyan, P. (2001). Extending slow manifolds near transcritical and pitchfork singularities. *Nonlinearity*, *14*(6): 1473–1491.

Krupa, M. and Wechselberger, M. (2010). Local analysis near a folded saddle-node singularity. *Journal of Differential Equations*, *248*(12): 2841–2888.

Kucera, D. R. and Orr, P. W. (1980). *Spruce Budworm in the Eastern United States. Forest Insect & Disease Leaflet 160.* Washington, DC: U.S. Department of Agriculture, Forest Service.

Ludwig, D., Jones, D. D., and Holling, C. S. (1978). Qualitative analysis of insect outbreak systems: The spruce budworm and forest. *The Journal of Animal Ecology*, *47*(1): 315–332.

Muratori, S. and Rinaldi, S. (1989). Catastrophic bifurcations in a second-order dynamical system with application to acid rain and forest collapse. *Applied Mathematical Modelling*, *13*(12): 674–681.

Pokrovskii, A., Shchepakina, E., and Sobolev, V. (2008). Canard doublet in a Lotka-Volterra type model. *Journal of Physics: Conference Series*, *138*(1): 012019.

Rinaldi, S. and Muratori, S. (1992). Limit cycles in slow-fast forest-pest models. *Theoretical Population Biology*, *41*(1): 26–43.

Schultz, M. (2009). Spruce Budworm. In G. Man (Ed.), *Major Forest Insect and Disease Conditions in the United States 2007*. Report *FS-919*, 38–40. Washington, DC: United States Department of Agriculture.

Szmolyan, P. and Wechselberger, M. (2001). Canards in $\mathbb{R}^3$. *Journal of Differential Equations*, *177*(2): 419–453.

Vo, T., Bertram, R., Tabak, J., et al. (2010). Mixed-mode oscillations as a mechanism for pseudo-plateau bursting. *Journal of Computational Neuroscience*, *28*(3): 443–458.

Wechselberger, M. (2005). Existence and bifurcation of canards in $\mathbb{R}^3$ in the case of a folded node. *SIAM Journal on Applied Dynamical Systems*, *4*(1): 101–139.